TORQUE RIPPLE AND MASS MINIMIZATION OF A 20-MW DIRECT DRIVE OFFSHORE WIND GENERATOR

Hoang Trung Kien*, Nguyen Thi Khanh Huyen

University of Science and Technology of Hanoi, Vietnam Academy of Science and Technology

*Corresponding author: hoang-trung.kien@usth.edu.vn

(Received: July 25, 2022; Accepted: September 6, 2022)

Abstract - This article investigates the structural optimization of a 20-MW offshore wind generator to minimize the torque ripple and mass. The surface-mounted permanent magnet topology will be chosen for the generator. In addition, the double-layer armature winding configuration will be utilized. The direct-drive technology will be adopted to increase the reliability of the offshore wind energy conversion system. The multi-objective optimization of the generator is carried out based on the particle swarm algorithm. Results show that the torque ripple of the optimal model is significantly reduced to as much as 0.41% at full-load conditions making the configuration suitable for the high-power offshore wind generator.

Key words - Offshore wind; optimization; permanent magnet wind generator; torque ripple

1. Introduction

Renewable energy has witnessed booming growth recently in various countries as a response to balancing their prosperity and decarbonization goals, setting the world towards achieving the Paris Agreement by 2050. Wind power is one of the fastest-growing renewable technologies, with the global installed capacity expanded nearly 100 times in just two decades, from 6.5 GW in 1997 to 743 GW in 2020. Onshore wind dominates offshore wind in terms of installed capacity, accounting for nearly 95% wind market [1]. However, the future capacity of onshore wind farms is constrained due to land restrictions and transmission congestion. Therefore, offshore wind appears as a complementary alternative thanks to the installed area's availability and fewer surrounding obstacles.

Wind turbines with higher nominal power are gaining increased attention to lower the cost of energy as the number of turbines will be reduced for the same wind farm's size (installed capacity). However, this will present new challenges in production, installation, and maintenance as well [2].

Permanent magnet synchronous generators (PMSGs) have become the dominant technologies for medium and larger wind turbines thanks to their efficiency, low maintenance cost, and high-power density. Although the turbine capacity is increasing rapidly, research for PMSG having rated power above 10-MW is gaining more research attention [3-6]. As of 2021, the largest commercial turbine, launching in 2024, is recorded to be 16-MW [7]. In addition, direct-drive wind generators are preferable as troubles associated with gearboxes are removed, and the system's reliability will be increased as a consequence. The drawback of this technology is that the generator's shaft speed is low (the same as the blade's speed), at high nominal power, this speed is getting lower as there is a limit on the tip speed of the blade. At low speed, the problem of torque ripple, which is defined as the variation of the torque around its mean value, is getting worse. As torque ripple is one of the essential factors in high-performance applications such as PMSG, its direct consequences, including vibration, acoustic noises, and friction on the generator [8] can decrease the turbine's performance and limit its lifespan [9].

Several researches are focusing on the torque ripple of wind generators with permanent magnets (PMs). Torque ripple reduction for small-scale wind generators was discussed in [10] by removing the DC-side capacitor and controlling the DC-side current to a constant value. However, the structural design of the generator was not taken into account. Dutta et al. presented cogging torque and torque ripple for a small power interior PM wind generator using different PM shapes. In [11], the authors investigated the torque ripple of an interior PMSG at 5.6 MW using slitting and skewing techniques. Nevertheless, using the interior PM type will cause a higher torque ripple due to the difference in the direct and quadrature axis inductances. A special type of PMSG is discussed and compared with a conventional type in [12] to improve the mean torque for direct-drive offshore wind applications. However, generators were not carefully designed to tackle torque ripple. A 4.5 MW PMSG was analyzed in [13]. Torque ripple was reduced by only considering a suitable PM shape.

In this research, a 20-MW PMSG and its torque ripple minimization by appropriate structural designs are investigated. In addition, for offshore wind generators at multi-megawatt power, the mass of the generator is of importance to lower the load on the turbine's tower and foundation. Therefore, together with the torque ripple reduction, the generator's active mass will be minimized at the same time to form a multi-objective optimization problem. Various structural aspects will be taken into consideration. The choice of that high nominal power is that it matches the trend of increasing nominal power for offshore wind turbines and it is believed to be in the optimal range to minimize the levelized cost of energy [14]. The generator will be described and optimized using the Particle Swarm Optimization (PSO) algorithm. The main contribution of this article is to analyze the performance in terms of torque ripple and mass of a 20-MW direct-drive wind generator by tackling its structural design, which has not been comprehensively done so far.

2. Methodology

2.1. PMSG configuration

The configuration considered in this study is a radial flux machine, whose magnetic flux direction is perpendicular to the machine's axis. The radial type is advantageous in terms of higher torque density, and the resistance to temperature demagnetization can be enhanced thanks to the improved cooling condition due to the rotor's direct exposure to the wind [15]. For this type, the placement of magnets can be categorized into two types: surface-mounted and interior. While the surface-mounted PMSG (SM-PMSG) is known to have lower torque ripple and causes less noise production [16], the interior PMSG (I-PMSG) has a higher power factor and less copper loss [17]. The SM-PMSG is most suitable for larger wind turbines for achieving the highest efficiency [18]. This research focuses on the performance evaluation of a double-layer SM-PMSG. This configuration is advantageous for direct-drive wind generators in terms of weight, cost, and torque ripple [19-22]. To minimize the 5th and 7th harmonics, the pitch factor is chosen as 5/6. The model to be simulated and optimized is shown in Figure 1.

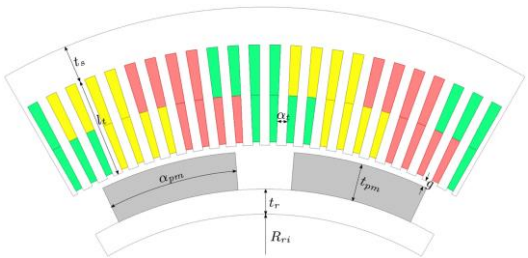

Figure 1. *Surface-mounted PMSG model*

Some main design parameters of the generator are described in Table 1, including fixed and dependent parameters. The rare earth permanent magnet with the residual flux density B_r = 1.1 T will be used. The non-linear core material with the magnetization curve is displayed in Figure 2, this material is used for both stator and rotor. The latter is calculated based on the former and related equations. The rated power can be calculated as

$$P_{nom} = \frac{1}{2} C_p(\lambda, \beta) \rho_{air} \pi R_{blade}^2 v_{nom}^3 \quad (1)$$

Table 1. *Main generator's design parameters*

Parameters	Description	Value
v_{nom}	Rated wind speed	11.4 m/s
ρ_{air}	Air density	1.225 kg/m^3
P_{nom}	Rated power	20 MW
C_p	Power coefficient	0.48
R_{blade}	Blade length	120.9 m
λ	Tip speed ratio	7
ω_{shaft}	Shaft speed	6.303 rpm
U_p	Rated line-to-line voltage	3.3
I_{rms}	Phase current (RMS)	3499 A
k_{fill}	Filling factor	0.65

where C_p is the power coefficient, which is chosen as 0.48 to maximize the capture power from wind, λ is the tip speed ratio which is chosen as 7.

From equation (1), the blade length R_{blade} can be deduced and the shaft speed, which is the same as the speed of the generator thanks to the direct-drive configuration, can be computed based on the tip speed ratio equation.

$$\lambda = \frac{w R_{blade}}{v_{nom}} \quad (2)$$

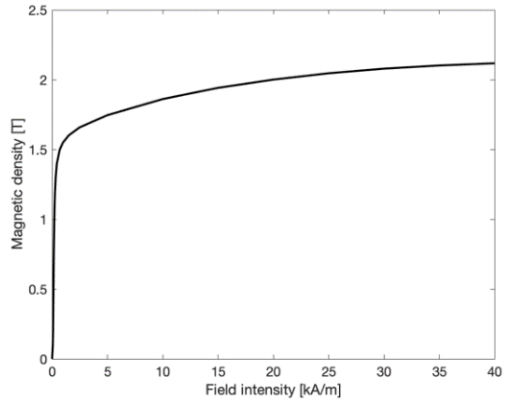

Figure 2. *Non-linear magnetization curve of the material used in the stator and rotor*

Nine variables, shown in Table 2, will be treated simultaneously using Particle Swarm Optimization (PSO) method. It is important to note in this article that, only overall structural variables are considered. Local variables such as a slight modification of the stator tooth tips are not taken into consideration as they have almost no impact on the generator's mass and are hard to be involved in the optimization. They are good to consider later on after the overall generator's structure is determined. Other techniques such as skewing or Halbach array magnet arrangement are not considered as well for the same reason. These special techniques can be accomplished at the expense of increasing manufacturing costs.

Table 2. *Optimization variables*

No.	Variables	Description
1	p	Number of pole pairs
2	N_a	Number of armature winding's turns
3	R_i	Shaft radius
4	t_r	Rotor yoke height
5	t_{pm}	PM height
6	α_{pm}	PM arc ratio
7	l_t	Stator tooth height
8	α_t	Tooth width ratio
9	t_s	Stator yoke height

2.2. Torque ripple

The instantaneous torque of an electrical machine consists of two components: the mean torque and the periodic component, which is a function depending on time or the rotor's position, superimposed on the former one [23].

Torque pulsation or torque ripple is a product of the periodic component and is commonly determined as the ratio between the difference between maximum and minimum torque values over the average one, as in equation (3) [23].

$$T_{ripple} = \frac{T_{max} - T_{min}}{T_{mean}} . 100\% \quad (3)$$

where T_{max}, T_{min}, and T_{mean} are the maximum, minimum,

and mean values of the torque profile.

Torque ripple in SM-PMSGs can be decomposed into two main components: load-independent cogging torque, resulting from the reciprocal action between the permanent magnet (PM)'s excitation magnetic field and the stator slot [24], and load-dependent torque pulsation, originating from the harmonic component of armature current and back-EMF [25]. Cogging torque is one of the essential factors in wind turbines, especially in high-performance applications such as SM-PMSG, since it creates vibration, acoustic noises, and friction on the generator, preventing the turbine from rotating at low speeds [8], decreasing its performance and limiting its lifespan [9].

2.3. Optimization algorithm

In this article, the Particle Swarm Optimization (PSO) algorithm will be used for torque minimization. The PSO, which was first introduced in 1995 [26], is a type of stochastic optimization method that originated via a simulation model studying the bird's flock or fish school movement.

Generally, PSO and genetic algorithm (GA) are two popular methods for optimizations thanks to their advantages of gradient-free and ability to find global optima [27]. In comparison with GA, PSO has a better performance in terms of accuracy, robustness, and especially less simulation time due to the faster convergence of PSO. The last aspect is the main reason to choose PSO in this article since optimization with finite element methods (FEM), which will be used for the machine's analyses, is very time-consuming.

Each particle in PSO serves as a potential solution to the optimization problem, where it can follow its own as well as the population's optimal position and velocity. Each individual is assigned a fitness value, and its new position and velocity are calculated based on this fitness value. The individual's states will be constantly adapted inside the multi-dimensional search space until the balance or optimal condition is achieved [28, 29]. The algorithm terminates only when the swarm radius falls below a specific small positive constant or the maximum number of iterations is reached [30]. The process of updating the particles' velocity and position at iteration n + 1 is manipulated by equations 4 and 5, respectively.

$$v_{id}{}^{n+1} = w v_{id}{}^{n} + c_1 r_1{}^{n}(p_{id}{}^{n} - x_{id}{}^{n}) + c_2 r_2{}^{n}\left(p_{gd}{}^{n} - x_{id}{}^{n}\right) \quad (4)$$

$$x_{id}{}^{n+1} = x_{id}{}^{n} + v_{id}{}^{n+1} \quad (5)$$

where w is the inertial weight constant, r_1 and r_2 are two uniformly distributed random numbers in the range [0, 1]. c_1 and c_2 are constants that control the effect of the personal and global guides. p_{id} and p_{gd} are personal best and global best, respectively. In this work, c_1 and c_2 are 1 and w is 0.8.

Each particle's optimal position, p_{id}, is selected after comparing the current position and the former optimal position while the swarm's optimal solution, p_{gd}, is decided based on the set of non-dominated solutions updated in the previous stage. The flowchart of the PSO algorithm is shown in Figure 3.

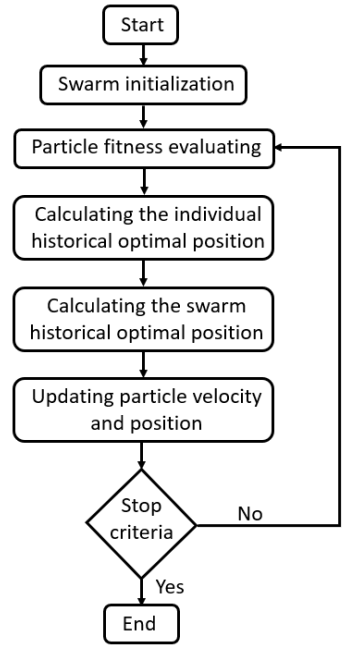

Figure 3. *PSO algorithm flowchart [29]*

3. Results and discussion

The generators are modeled by 2-D FEM using ANSYS Maxwell coupled with MATLAB for optimization. Generators are optimized to minimize the mass torque ripple at the rated power. The optimization problem is formulated in equation 6. In this equation, the current density of the PMSG's armature winding must be smaller than J_{max} which is set at 6 A/mm^2 [31].

$$\begin{aligned} &\underset{X_{PMSG}}{\text{minimize}}\, f(X_{PMSG}) = \begin{cases} Mass \\ Torque\ ripple \end{cases} \\ &X_{PMSG} = (P, N_a, R_i, t_r, t_{pm}, \alpha_{pm}, l_t, \alpha_t, t_s) \\ &\text{s.t. } P_{gen} \geq P_{nom}, J \leq 6\ A/mm^2 \end{aligned} \quad (6)$$

The two optimization objectives i.e., the generator's mass and torque ripple are contradictory in the sense that to lower the torque ripple the generator's mass might be bigger. For example, a bigger magnetic air gap will lower and reduce the torque ripple as it can mitigate the sudden change in the flux density distribution. However bigger air gap increases the overall volume and hence the mass of the generator. In addition, more PM is required to maintain the air-gap flux density, this makes the overall mass increase.

As cogging torque is a particularly important component of the torque ripple. The impacts of some optimization variables on the cogging torque will be investigated first. Among optimization variables, the stator tooth width and PM arc ratio are of importance since they are associated with the slot opening and directly influence the flux density distribution in the generator's air gap. For this reason, an elaborate analysis of these two factors will be carried out. Other structural variables are more clearly related to the generator's mass but not the torque ripple. For example, increasing the length of the stator tooth will hardly change the torque ripple but give more room for the stator winding which helps lower the current density and increases the overall generator's mass. The stator and rotor yoke height do

not have noticeable impacts on the torque quality as their main functions are to conduct the flux, and as long as they are not highly saturated the air-gap flux density distribution is almost independent of their thickness. But still, combinations of them should impact the torque quality.

The torque ripple can be minimized as a consequence of changing the relative PM width and the slot opening width. The decrease in slot opening width can lead to a dilemma on the cogging torque amplitude. A narrower slot opening can smooth the air-gap permeance variation due to a decrease in the slotting effect, lowering the cogging torque. On the other hand, the air-gap permeance variation can be escalated due to the local magnetic saturation enhanced by tooth-tip leakage flux when slot opening width is reduced, resulting in higher cogging torque. In contrast, the variation of air-gap permeance becomes larger when the slot opening is wider, resulting in higher cogging torque and torque ripple [32]. Besides, a wider slot opening also affects the value of relative PM width having the lowest ripple level. The harmonics of the air-gap flux will increase with the increase of slot opening width, and the interaction between these harmonics and the space harmonics in the magneto-motive force will create an addition in the cogging torque and contribute to the torque ripple at load conditions. If the PM geometry is well assigned, the ripple created by the latter harmonic component can make up for the cogging torque, leading to a lower torque. Therefore, different load conditions will lead to a change in saturation, making the optimal design for minimum cogging torque cannot guarantee obtaining the minimum on-load torque ripple and vice versa [33].

Table 3. *Variables for the impact analysis of the tooth width and PM arc ratios*

No.	Variables	Value
1	p	22
2	N_a	2
3	R_i	3.516 m
4	t_r	0.106 m
5	t_{pm}	0.157 m
6	α_{pm}	0.1 ÷ 0.9
7	l_t	0.317 m
8	α_t	0.1 ÷ 0.9
9	t_s	0.108

In order to explore the impact of PM arc ratio and stator tooth width on the cogging torque, these two variables will be varied from 0.1 to 0.9 independently, other variables will be kept constant, and the generator is disconnected from the load i.e., the stator current is null. lists the variable with their values for this analysis. It is noted that those values are just chosen arbitrarily. When the tooth width ratio varies from 0.1 to 0.9, the PM arc ratio remains the same at 0.5, and when the PM arc ratio changes from 0.1 to 0.9, the tooth width ratio is fixed at 0.5, similarly. Figure 4 and Figure 5 illustrate the influences of the stator tooth width and PM arc ratio, respectively. As it can be seen, increasing the stator tooth width increases the cogging torque. It seems to expect that a narrow stator tooth is preferable considering a low cogging torque, however, a narrow tooth will experience a strong saturation at load conditions. The cogging torque when changing the PM arc ratio peaks at the PM arc takes up 50% of the pole (at the condition that the stator tooth width equals the slot opening).

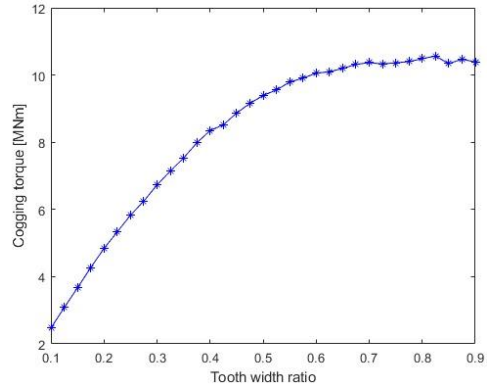

Figure 4. *Impact of the stator tooth width on the cogging torque*

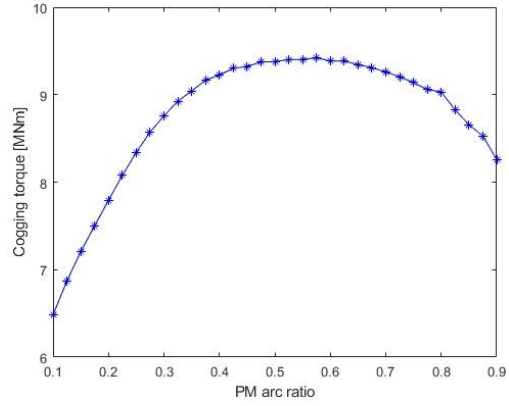

Figure 5. *Impact of the PM arc ratio on the cogging torque*

The optimization result is displayed in Figure 6 in form of the non-dominated pareto-front. The numbers of particles and iterations are set to 300 and 50, respectively. There are 27 optimal points presented in the pareto-front set. Generally, it can be seen from Figure 6 that the torque ripple can be reduced to as much as 0.41%. On these pareto-front results, three specific generators (marked in Figure 6), will be extracted for further investigations. Two generators at the extreme points of the pareto-front (lowest torque ripple and lowest mass), one generator just at the middle (generator numbered 14th). The three generators are shown in Figure 7 with the detailed design parameters of those generators are presented in Table 4.

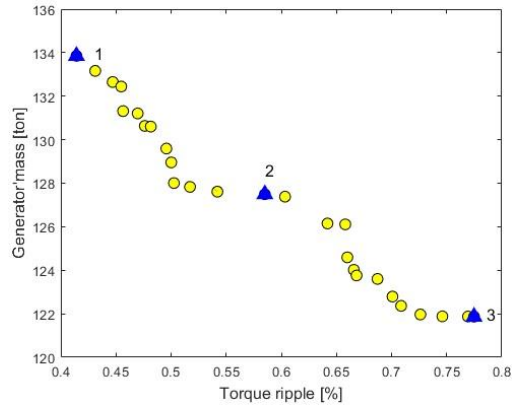

Figure 6. *Non-dominated pareto-front of the optimization result*

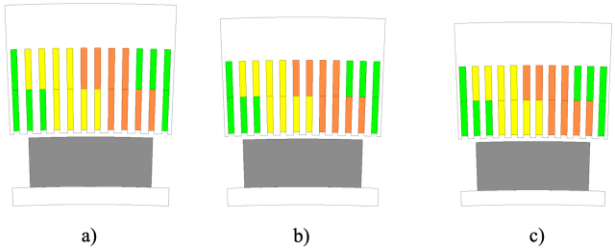

Figure 7. *Three generators (one pole), extracted in Figure 6: a) Generator 1, b) Generator 2, c) Generator 3*

Table 4. *Design parameters of the three extracted generators in Figure 6*

Variables	Unit	Gen. 1	Gen. 2	Gen. 3
p	–	38	38	40
N_a	–	1	1	1
R_i	m	3.815	3.800	3.803
t_r	m	0.036	0.037	0.030
t_{pm}	m	0.1	0.1	0.1
α_{pm}	–	0.771	0.770	0.768
l_t	m	0.171	0.156	0.150
α_t	–	0.592	0.551	0.504
t_s	m	0.09	0.09	0.09
Stack length	m	1.859	1.852	1.850
Power	MW	20.02	20.01	20.01
Mass	ton	133.9	127.5	121.9
Torque ripple	%	0.41	0.59	0.77

As it can be seen, the number of pole pairs tends to converge to a large number which around 40 to reduce the torque ripple, which is generally true. The tooth width ratio seems to stay around 0.55, as already stated earlier, it can be as compromised between the low cogging torque and current density limits. It is interesting to observe that the PM arc ratio tends to remain at about 0.77 which is also at a high cogging torque region as demonstrated in Figure 5. However, similarly to the tooth width ratio, a high PM ratio is required to maintain the power capability of the generator.

The torque ripple profiles of the three generators are demonstrated in Figure 8. The torques are remarkably close regarding the mean value, which is 30.3 MNm, this is due to the same power constraint of 20 MW applied to all generators.

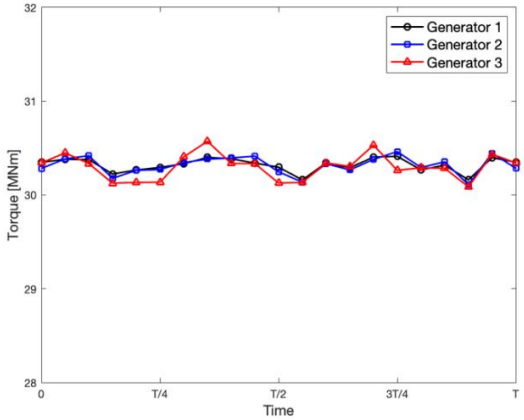

Figure 8. *Torque ripple comparison of the three extracted generators*

Cogging torque comparison of the three generators is displayed in Figure 9. It is interesting to observe that even the generator 1 has the lowest torque ripple but the cogging torque of this generator is highest. The cogging torque, presented as the percentage of the mean torque is also computed, the results reveal a very low value compared to the recommended ratio of 2% as noted in [19]. The no-load voltages of the three generators are shown in Figure 10. As it can be seen, the third harmonics is pretty high, contributing the total harmonic distortion of about 8.4%. However, the generator is interfaced with the grid via full-scale back-to-back converter, so that this harmonic is not an issue.

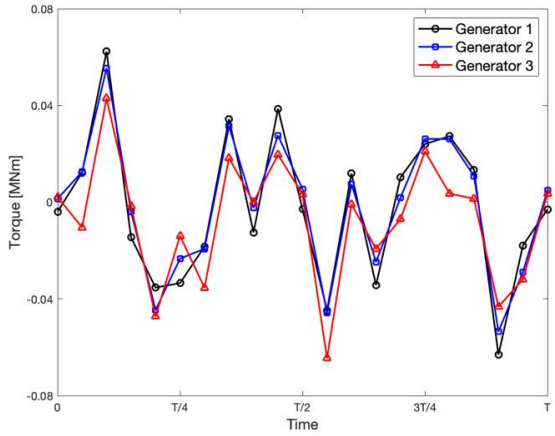

Figure 9. *Cogging torque comparison of the three extracted generators*

The cogging torques of the three generators are summarized in Table 5.

Table 5. *Cogging torque of the three extracted generators*

	Gen. 1	Gen. 2	Gen. 3
Cogging torque [kNm]	62.73	54.46	53.73
Cogging torque [% of the rated torque]	0.21	0.18	0.18

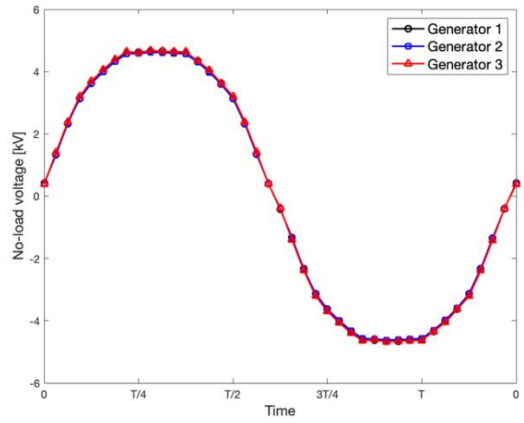

Figure 10. *No-load voltage of the three extracted generators*

4. Conclusion

The multi-objective optimization of a direct-drive wind generator at 20 MW has been performed targeting both the generator mass and torque ripple. With the surface-mounted PM topology together with a good winding configuration (by choosing a pitch factor of 5/6), the torque ripple could be reduced to as much as 0.41% at the full-load condition. The result is remarkably interesting to explore the use of

very high-power turbines (causing a low shaft speed) for offshore applications since the torque ripple can severely degrade the performance of the generator at low speed. In this work, rare earth permanent magnets were used, which makes the generator expensive. In future work, a comparison between ferrite and rare earth permanent magnets for the generator will be co`nducted. Additionally, some special techniques to further reduce the torque ripple without influencing the generator's mass will be considered such as skewing or Halbach array magnet arrangement.

Acknowledgement: This research is funded by the University of Science and Technology of Hanoi under grant number USTH.EN.01/22.

REFERENCES

[1] GWEC, "*Global wind report 2021*" Global Wind Energy Council, Tech. Rep., 2021.

[2] G. A. M. van Kuik, "*Long-term research challenges in wind energy - a research agenda by the European Academy of wind energy*", Wind Energy, 2016.

[3] C. Stuebig, A. Seibel, K. Schleicher, L. Haberjan, M. Kloepzig, and B. Ponick, "Electromagnetic design of a 10 MW permanent magnet synchronous generator for wind turbine application*", in 2015 IEEE International Electric Machines & Drives Conference (IEMDC),* 2015, pp. 1202–1208.

[4] D. Liu, H. Polinder, A. B. Abrahamsen, and J. A. Ferreira, "Comparison of 10 MW superconducting generator topologies for direct-drive wind turbines", *in 2015 IEEE International Electric Machines Drives Conference (IEMDC),* May 2015, pp. 174–180.

[5] M. Shafiee, F. Brennan, and I. A. Espinosa, "A parametric whole life cost model for offshore wind farms", *The International Journal of Life Cycle Assessment,* vol. 21, 2016, pp. 961–975.

[6] F. K. Moghadam and A. R. Nejad, *"Evaluation of PMSG-based drivetrain technologies for 10 MW floating offshore wind turbines: Pros and cons in a life cycle perspective",* Wind Energy, 2020.

[7] L. B. K. Fisch and M. L. Heldwein, "10-MW direct-drive PMSG-based wind energy conversion system model", *in 2020 IEEE 21st Workshop on Control and Modeling for Power Electronics (COMPEL),* 2020, pp. 1–8.

[8] Y. Yasa and E. Mese, "Design and analysis of generator and converters for outer rotor direct drive gearless small-scale wind turbines", *in 2014 International Conference on Renewable Energy Research and Application (ICRERA),* 2014, pp. 689–694.

[9] W. Q. Chu and Z. Q. Zhu, "Investigation of torque ripples in permanent magnet synchronous machines with skewing", *IEEE Transactions on Magnetics,* vol. 49, no. 3, pp. 1211–1220, 2013.

[10] Y.Y.Xia, J.E.Fletcher, S.J.Finney, K.H.Ahmed, and B.W.Williams, *"Torque ripple analysis and reduction for wind energy conversion systems using an uncontrolled rectifier and boost converter",* IET Renewable Power Generation, 2011.

[11] D. Lee, C.-G. Lee, Y.-J. Kim, and S.-Y. Jung, "Numerical design characteristics of interior permanent magnet synchronous generator for offshore wind turbines", *in 9th IET International Conference on Computation in Electromagnetics (CEM 2014),* 2014, pp. 1–2.

[12] D. K. K. Padinharu, G.-J. Li, Z.-Q. Zhu, R. Clark, A. S. Thomas, and Z. Azar, "System-level investigation of multi-MW direct-drive wind power pm vernier generators", *IEEE Access,* vol. 8, pp. 191 433–191 446, 2020.

[13] H.Hao, W.zhong Fei, D.min Miao, M.jiaJin, and J.xinShen,"Torque characteristics in a large permanent magnet synchronous generator with stator radial ventilating air ducts", *Frontiers of Information Technology & Electronic Engineering,* vol. 17, pp. 814–824, 2016.

[14] T.-K. Hoang, L. Queval, L. Vido, and C. Berriaud, "Impact of the rotor blade technology on the levelized cost of energy of an offshore wind turbine", *in 2017 International Conference on Optimization of Electrical and Electronic Equipment (OPTIM) & 2017 Intl Aegean Conference on Electrical Machines and Power Electronics (ACEMP),* 2017, pp. 623–629.

[15] R. Rashmi, V. Ramanujan, and M. Purushotham, "Permanent magnet synchronous generator configuration in wind turbines - technological status review, survey and market trends", *International Journal of Scientific & Engineering Research,* vol. 6, 2015, pp. 23 – 30.

[16] P.Roshanfekr, T.Thiringer, M.Alatalo, and S.Lundmark, "Performance of two 5 MW permanent magnet wind turbine generators using surface mounted and interior mounted magnets", *in 2012 XXth International Conference on Electrical Machines,* 2012, pp. 1041–1047.

[17] H. Karimi-Davijani and O. Ojo, "Optimum control of grid connected interior permanent magnet wind turbine generator," *2012 IEEE Energy Conversion Congress and Exposition (ECCE),* 2012, pp. 3764-3771.

[18] H. Haraguchi, S. Morimoto, and M. Sanada, "Suitable design of a PMSG for a small-scale wind power generator*", in 2009 International Conference on Electrical Machines and Systems,* 2009, pp. 1–6.

[19] M. Popescu, M. V. Cistelecan, L. Melcescu, and M. Covrig, "Low speed directly driven permanent magnet synchronous generators for wind energy applications", *in 2007 International Conference on Clean Electrical Power,* May 2007, pp. 784–788.

[20] H.Chen, R.Qu, J.Li, and B.Zhao, "Comparison of interior and surface permanent magnet machines with fractional slot concentrated windings for direct-drive wind generators", *in 2014 17th International Conference on Electrical Machines and Systems (ICEMS),* Oct 2014, pp. 2612–2617.

[21] A. McDonald and N. A. Bhuiyan, "On the optimization of generators for offshore direct drive wind turbines", *IEEE Transactions on Energy Conversion,* vol. 32, no. 1, March 2017, pp. 348–358.

[22] L. Frosini and M. Pastura, "Analysis and design of innovative magnetic wedges for high-efficiency permanent magnet synchronous machines", *Energies,* vol. 13, no. 1, 2020, pp. 1-21.

[23] J.F.Gieras, C.Wang, and J.C.Lai, *Noise of Polyphase Electric Motors.* Taylor & Francis CRC Press, 2005.

[24] Herlina, R. Setiabudy, and A. Rahardjo, *"Cogging torque reduction by modifying stator teeth and permanent magnet shape on a surface mounted PMSG",* in 2017 International Seminar on Intelligent Technology and Its Applications (ISITIA), 2017, pp. 227–232.

[25] W. Fei and P. C.-K. Luk, "Torque ripple reduction of a direct-drive permanent-magnet synchronous machine by material-efficient axial pole pairing", *IEEE Transactions on Industrial Electronics,* vol. 59, no. 6, 2012, pp. 2601–2611.

[26] J. Kennedy and R. Eberhart, "Particle swarm optimization", *in Proceedings of ICNN'95 - International Conference on Neural Networks,* vol. 4, 1995, pp. 1942–1948.

[27] Y. Duan, R. G. Harley and T. G. Habetler, "Comparison of Particle Swarm Optimization and Genetic Algorithm in the design of permanent magnet motors", *2009 IEEE 6th International Power Electronics and Motion Control Conference,* 2009, pp. 822-825, doi: 10.1109/IPEMC.2009.5157497.

[28] M. J. Reddy and D. N. Kumar, "*Multi-objective particle swarm optimization* for generating optimal trade-offs in reservoir operation", Hydrological Processes, 2007.

[29] D. Wang, D. Tan, and L. Liu, "Particle swarm optimization algorithm: an overview", *Soft computing,* vol. 22, 2018, pp. 387–408.

[30] U. Baumgartner, C. Magele, and W. Renhart, "Pareto optimality and particle swarm optimization", *IEEE Transactions on Magnetics,* vol. 40, no. 2, 2004, pp. 1172–1175.

[31] L.Sethuraman, M.Maness, and K.Dykes, *"Optimized generator designs for the DTU 10-MW offshore wind turbine using generatorSE",* National Renewable Energy Laboratory, Tech. Rep., Jan. 2017.

[32] Z. Zhu and D. Howe, "Influence of design parameters on cogging torque in permanent magnet machines", *IEEE Transactions on Energy Conversion,* vol. 15, no. 4, pp. 407–412, 2000.

[33] D.Wu and Z.Zhu, "Design trade-off between cogging torque and torque ripple in fractional slot surface-mounted permanent magnet machines", *in 2015 IEEE International Magnetics Conference (INTERMAG),* 2015, pp. 1–1.